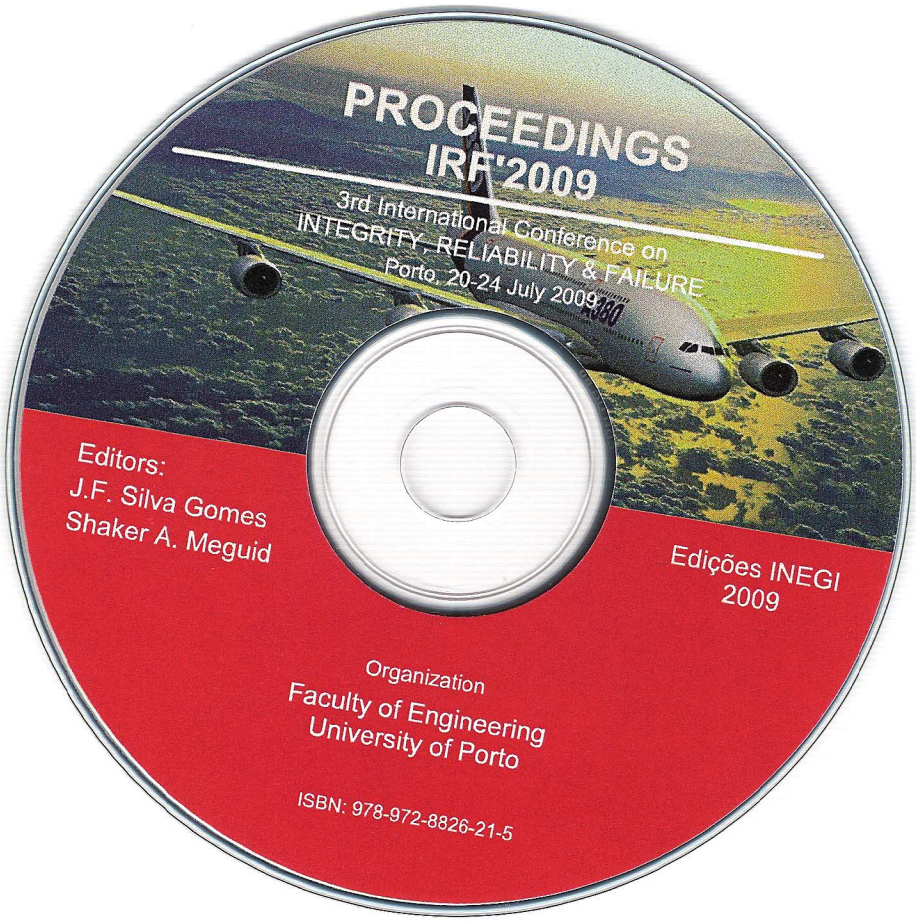
PROCEEDINGS
IRF'2009
3rd International Conference on
INTEGRITY, RELIABILITY & FAILURE
Porto, 20-24 July 2009
Editors:
J.F. Silva Gomes
Shaker A. Meguid
Edições INEGI
2009
Organization
Faculty of Engineering
University of Porto
ISBN: 978-972-8826-21-5

HUMAN FEMUR ASSESSMENT USING ISOTROPIC AND ORTHOTROPIC MATERIALS DEPENDENT OF BONE DENSITY

E.M.M. FONSECA, M.J.LIMA, L.M.S. BARREIRA
Polytechnic Institute of Bragança
Bragança, Portugal,
Email: efonseca@ipb.pt

SYNOPSIS

The bone mass reduction and the deterioration of the tissue micron-architecture lead to a bigger fragility of the bone and to the consequent increase of the fracture risk. For this fact, it is considered excellent the quantification of the mass density and the verification of its influence in the bone resistance assessment. The apparent density is defined as the density without fluid influence, being the effective density at that includes the marrow mass, essentially fluid. This measurement is made through the use of a gray scale values on the medical image in study. The values in Hounsfield units are determined, being this scale later converted into measure of the bone density. With this measure an exponential relation will be used allowing calculate the biomechanics properties dependence for cortical and trabecular bone. With this work it is intended to assessment the susceptible weak zones, for a human femur with 70 years old, using the finite element method through ANSYS® program. The main objective is obtaining the stresses distributions, using different values of bone density and their relation with exponential laws for isotropic and orthotropic materials properties.

INTRODUCTION

The finite element method has been used in biomechanics studies through the simulation of some anatomical structures. Some authors have come to dedicate their works in this area, through numerical simulations of human femur using solid models (Baca, 2008), (Taylor, 1996), for example. Also, in the experimental area, they have been published results from (Bergmann, 2001), (Simões, 2004). Some authors, (Baca, 2008), (Peng, 2006), have used different numerical simulations with isotropic and orthotropic constituent models, for bone tissues. The biomechanics properties depend on structural aspects of the bone, its bone geometry, but also on intrinsic properties of the material, between which, the bone density. Particularly, the bone density keeps one strong inverse relation with the risk of bone fracture (Augat, 2006). The objective of this work is to produce one numerical femur model, constituted of different cortical and trabecular bone layers, through the effective density measurement under medical image. The study will be developed with the previous medical image treatment, gotten of one male femur with 70 years old. Pre-processing and treatment techniques were used for the study of medical image. The femur model is converted into 3D CAD format being later used in a biomechanics numerical simulation. It is intended thus, to present a methodology of scientific interest that allows evaluating the different results that if they get in function of bone density variation for an anatomical structure when different materials properties were used.

METHODS AND MATERIALS

The determination of bone properties require a carefully analysis through the medical image study (Kourtis, 2008). The gray values of the computerized tomography (CT) show the quantity of the absorbed radiation by the body parts in analysis. More dense tissues absorb more radiation than lesser dense, in X-rays form. This type of colours and densities produce the final medical image. For each medical image pixel, corresponds a medium value of tissues absorbed in this zone, defined in Hounsfield units (HU). The Hounsfield unit scale is a linear transformation of the linear attenuation coefficient measurement, following the expression (Kourtis, 2008):

$$HU = 1000 \frac{\mu_{tissue} - \mu_{water}}{\mu_{water} - \mu_{air}} \quad (1)$$

where μ_{tissue} is the linear attenuation value of the target tissue, μ_{water} is the linear attenuation coefficient for water and μ_{air} is the linear attenuation coefficient for air (typically assumed to be 0). In the case of clinical medical image (CT), the gray scale values correspond to HU, and equation 1 is not necessary (Kourtis, 2008).
There are some published values of Hounsfield, table 1, obtained in DICOM medical images.

Table 1: Typical values of HU. web page: //en.wikipedia.org

Substance	HU
Implant	>1000
Bone	400 a 1000
White material	46
Gray material	43
Blood	40
Muscle	10 a 40
Water	0
Fat	-100 a -50
Air	-1000

The studied male femur (M) has 70 years old. It is a right femur with a body mass of 70kg. Different numerical analyses were produced to compare the final solution with different bone density variation. For the global proximal femur model in study, the ranges of the measured HU were divided in different femur parts. Figure 1 represents different femur parts for tissue analysis, using CAD 3D image and CT images. The values obtained for each femur part were presented in table 2.

Table 2: Measured medium values of HU in CT image.

Femur part (M)	Cortical Bone	Trabecular Bone
Head (Zs)	563-499	45-265
Neck (Zi1)	614-878	
Body (Zi2)	1186-963	

The value range could be compared with a typical male bone structure observed by (Alho, 1989). The cortical density of the femur head is lesser when compared with the femur body part density, as registered by (Alho, 1989).

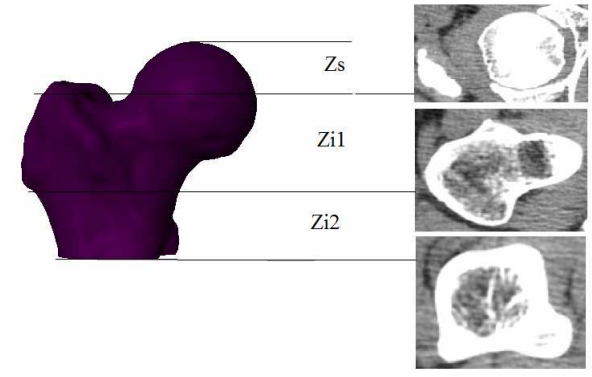

Fig. 1 Femur parts and CT images.

The effective bone density was calculated with the following equation, obtained by linear correlation, as reported in (Kourtis, 2008), (Baca, 2008):

$$\rho = 4.64 \times 10^{-4} \times HU + 1 \tag{2}$$

where ρ represent the effective density in g/cm^3 function of measured HU value.

MECHANICAL PROPERTIES OF BONE

The bone is a non homogeneous structure consisting, essentially, in two different types of materials, cortical and trabecular. In numerical biomechanical simulation, the bone material properties were assumed to be isotropic or orthotropic, for linear elastic. Different types of material properties were used for both models: isotropic homogenous (IH), two isotropic inhomogeneous (INH1 and INH2), orthotropic homogenous (OH) and two orthotropic inhomogeneous (ONH1 and ONH2). To consider the bone analysis, as a homogeneous or inhomogeneous structure, different simulations were made with different values of mechanical properties through bone tissue. The relations between bone and density are obtained with exponential equations, as reported by (Baca, 2008), (Peng, 2006). The following equations are used for isotropic bone properties:

$$E_c = 2065\rho^{3.09} \tag{3}$$

$$E_t = 1904\rho^{1.64} \tag{4}$$

where E is the elastic modulus for cortical or trabecular bone in MPa, function of bone density ρ in g/cm^3. The Possoin coefficient was assumed equal 0.3, for any bone tissues (Baca, 2008), (Peng, 2006), for isotropic bone properties.
In table 3, the properties of bone tissues for each isotropic model were represented. The values of these proprieties were obtained using equations 3 and 4 and registered values in table 2. For trabecular bone the same value of density was considered.

Table 3: Bone isotropic properties.

Bone tissue		Cortical		Trabecular	
Femur part		ρ, g/cm^3	E_c, MPa	ρ, g/cm^3	E_t, MPa
IH	Zs,Zi1,Zi2	1.39	5712.6	1.05	2062.6
INH1	Zs,Zi1	1.29	4535.7		
	Zi2	1.49	7080.5		
INH2	Zs	1.25	4115.0		
	Zi1	1.32	4869.6		
	Zi2	1.49	7080.5		

The expressions used for an orthotropic bone material are referred by (Baca, 2008), (Peng, 2006):

$$E_{1c} = E_{2c} = 2314\rho^{1.57},\ E_{3c} = 2065\rho^{3.09} \quad (5)$$

$$E_{1t} = E_{2t} = 1157\rho^{1.78},\ E_{3t} = 1904\rho^{1.64} \quad (6)$$

$$G_{12} = 5.71\rho^2/\rho_{\max}^2;\ G_{23} = 7.11\rho^2/\rho_{\max}^2;\ G_{31} = 6.58\rho^2/\rho_{\max}^2 \quad (7)$$

$$\nu_{12} = 0.4,\ \nu_{23} = \nu_{31} = 0.25 \quad (8)$$

where E is the elastic modulus for cortical or trabecular bone in MPa, function of bone density ρ in g/cm^3, G is the shear modulus in MPa and ν is Poisson ratio.
The orthotropic model was defined in the same way as the isotropic model, but using expressions 5-8.
Tables 4, 5 and 6 represent the values for all femur parts considered, in the studied case.

Table 4: Bone orthotropic properties for OH model.

Bone tissue	Cortical		Trabecular	
Femur part	ρ, g/cm^3	E_c, MPa	ρ, g/cm^3	E_t, MPa
Zs,Zi1,Zi2	1.39	E_1=3880.6 E_2=3880.6 E_3=5712.6 G_{12}=5.71 G_{23}=7.11 G_{31}=6.58 v_{12}=0.4 v_{23}=0.25 v_{31}=0.25	1.05	E_1=1262.0 E_2=1262.0 E_3=2062.6 G_{12}=5.71 G_{23}=7.11 G_{31}=6.58 v_{12}=0.4 v_{23}=0.25 v_{31}=0.25

Table 5: Bone orthotropic properties for ONH1 model.

Bone tissue	Cortical		Trabecular	
Femur part	ρ, g/cm^3	E_c, MPa	ρ, g/cm^3	E_t, MPa
Zs,Zi1	1.29	E_1=3451.4 E_2=3451.4 E_3=4535.7 G_{12}=4.28 G_{23}=5.33 G_{31}=4.93 v_{12}=0.4 v_{23}=0.25 v_{31}=0.25	1.05	E_1=1262.0 E_2=1262.0 E_3=2062.6 G_{12}=5.71 G_{23}=7.11 G_{31}=6.58 v_{12}=0.4 v_{23}=0.25 v_{31}=0.25
Zi2	1.49	E_1=4327.79 E_2=4327.79 E_3=7080.53 G_{12}=5.71 G_{23}=7.11 G_{31}=6.58 v_{12}=0.4 v_{23}=0.25 v_{31}=0.25		

Table 6: Bone orthotropic properties for ONH2 model.

Bone tissue	Cortical		Trabecular	
Femur part	ρ, g/cm^3	E_c, MPa	ρ, g/cm^3	E_t, MPa
Zs	1.25	E_1=3284.8 E_2=3284.8 E_3=4115.0 G_{12}=4.02 G_{23}=5.00 G_{31}=4.63 v_{12}=0.4 v_{23}=0.25 v_{31}=0.25	1.05	E_1=1262.0 E_2=1262.0 E_3=2062.6 G_{12}=5.71 G_{23}=7.11 G_{31}=6.58 v_{12}=0.4 v_{23}=0.25 v_{31}=0.25
Zi1	1.32	E_1=3578.2 E_2=3578.2 E_3=4869.6 G_{12}=4.48 G_{23}=5.58 G_{31}=5.16 v_{12}=0.4 v_{23}=0.25 v_{31}=0.25		
Zi2	1.49	E_1=4327.8 E_2=4327.8 E_3=7080.5 G_{12}=5.71 G_{23}=7.11 G_{31}=6.58 v_{12}=0.4 v_{23}=0.25 v_{31}=0.25		

FINITE ELEMENT MODEL

A finite element mesh was created based on a geometry obtained in STL format. This type of format was obtained through an image processing method in SCANIP® program. With STL format and using FEMAP® program, a solid mesh was generated with different masks to simulate trabecular and cortical bone. The analyses of finite element were made in ANSYS® program. Solid finite elements with six degrees of freedom were used.

In figure 2 two meshes of finite elements are presented, one for cortical bone and other for trabecular bone. A 3D and structural element finite element was choosing with 8 nodes and 3 degrees of freedom for each node.

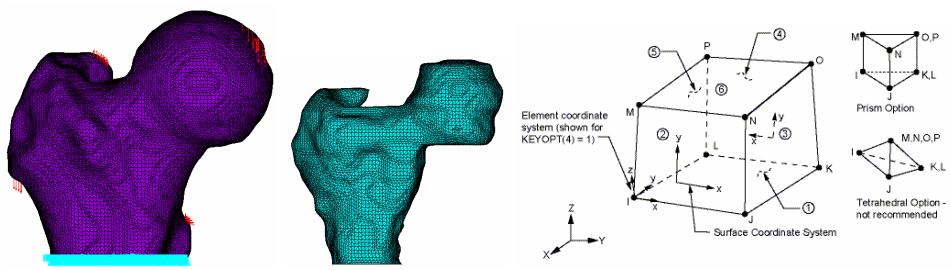

Fig. 2 Mesh used for cortical and trabecular bone with *Solid45*.

The main goal of this work was to analysis the femoral neck when submitted to different loading conditions. A joint reaction force was applied in the femoral head simultaneously with the influence of muscles forces. The principal muscle groups included in this work were the abductors, the ilio-tibial tract and iliopsoas. For the loading conditions, muscle and joint reaction forces were included in the numerical model. A joint reaction force of 1784N was imposed in the femur-acetabulum contact system at 35º in the transverse plane and at 12º in the coronal plane (Bergmann, 2001), which for an average mass of 70kg corresponds to 2.6 times body weight. The value of this load is according the activity of down stairs, as suggested by (Bergmann, 2001), where a collected gait data were recorded and measured in vivo. Muscles have the ability to absorb forces and distribute load, stabilize the structure and minimize the bending effort (Taylor, 1996). When the bone is loaded in bending, higher stresses are generated and more bone mass is required to resist them. If the bone is submitted to compression, lower stress levels and less bone mass is required. In this study the muscles loads considered were reported by (Taylor, 1996). Table 7 shows the values of the analysed load case.

Table 7: Loading condition imposed.

Load case	Resultant, N
Joint reaction force (Bergmann, 2001)	1784
Abductors (Taylor, 1996)	1237
Iliopsoas (Taylor, 1996)	771
Ilio-tibial tract (Taylor, 1996)	1200

Distal femur extremity was fixed, and axes body is parallel to global z in finite elements, according figure 2.

RESULTS AND DISCUSSION

Figure 3 represents the study of human femur using the finite element method. For results calculation, two anatomical plans were considered under different bone tissue densities. Horizontal plan (H) AMPL represents the zone of Anterior, Medial, Posterior and Lateral femur. The inclined plan (I), assigned for ADPPr, belongs to the Anterior, Distal, Posterior and Proximal zone femur.

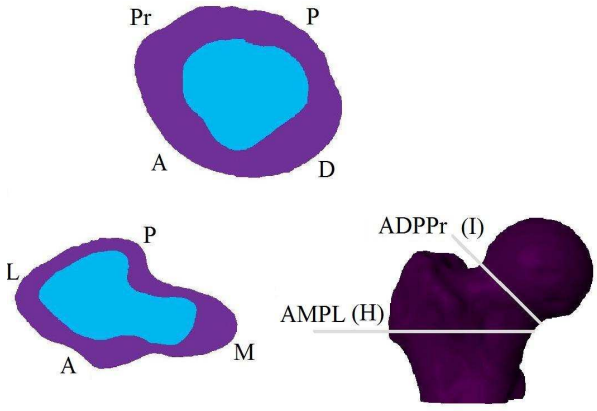

Fig. 3 Planes for results analysis, femur right side.

The results of equivalent stresses in (H) plane are represented in figure 4. In the medial femur part the stresses are more raised, being that the influence of the mechanical properties if reflects in the lateral femur zone. The orthotropic model realizes a more uniform stress distribution along (H) plane.

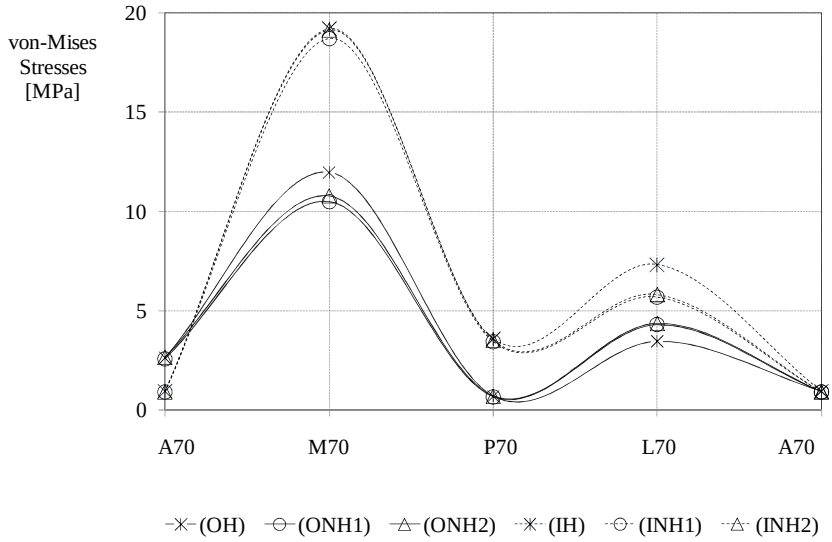

Fig. 4 Equivalent stresses in cortical zone (H).

In relation to (I) plane, the result of the equivalent stresses are represented in figure 5. A greater results influence exists when IH or OH models are used. Similar results are obtained with INH and ONH models.

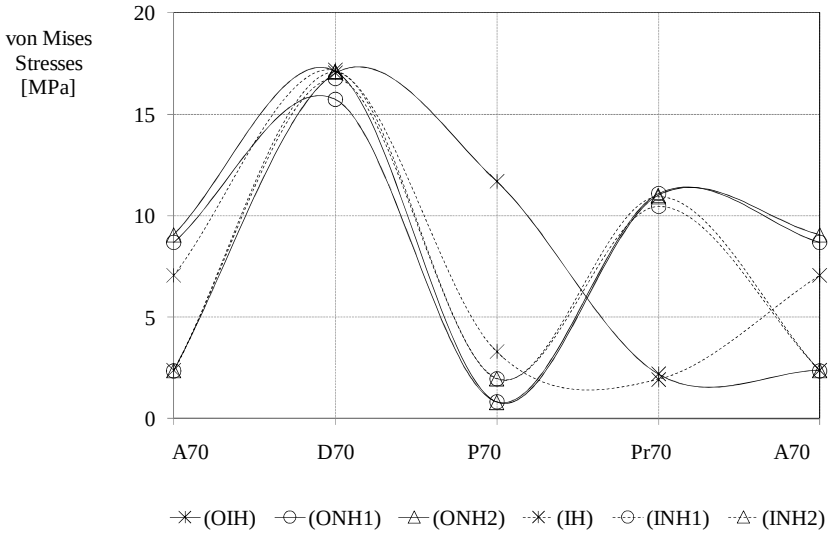

Fig. 5 Equivalent stresses in cortical zone (I).

Tables 8 and 9, represent the principal stresses (S1 maximum and S3 minimum stress value) for each studied femur zone. Different results were obtained for each model used (IH/OH, INH1/ONH1 and INH2/ONH2). Figures 6 and 7 show the evolution in tensile or compressive effect along each femur part in study.

Table 8: Principal stresses in horizontal plane (H), MPa.

	A		M		P		L	
	IH	**OH**	**IH**	**OH**	**IH**	**OH**	**IH**	**OH**
S1	0.173	1.447	-1.881	-6.032	2.999	0.139	5.686	2.561
S3	-0.884	-1.494	-22.607	-19.762	-0.877	-0.661	-1.381	-1.411
	INH1	**ONH1**	**INH1**	**ONH1**	**INH1**	**ONH1**	**INH1**	**ONH1**
S1	0.160	1.252	-1.779	-6.460	2.917	0.026	4.898	3.281
S3	-0.819	-1.576	-21.670	-18.559	-0.840	-0.744	-1.223	-1.575
	INH2	**ONH2**	**INH2**	**ONH2**	**INH2**	**ONH2**	**INH2**	**ONH2**
S1	0.159	1.291	-1.834	-6.905	2.969	0.042	5.027	3.354
S3	-0.825	-1.626	-22.209	-19.356	-0.863	-0.760	-1.229	-1.573

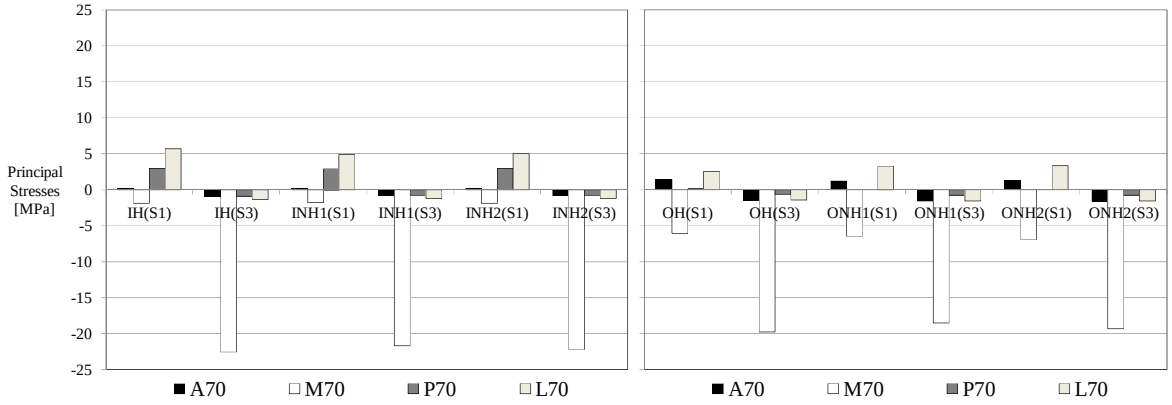

Fig. 6 Principal stresses in cortical zone (H) for isotropic and orthotropic model.

In table 8 or figure 6, a compressive state stress in medial femur part is visible. The values obtained with orthotropic model are lesser than the isotropic model. Homogeneous model (IH or OH) has different values in comparison with inhomogeneous models (INH or ONH).

Table 9: Principal stresses in inclined plane (I), MPa.

	A		D		P		Pr	
	IH	**OH**	**IH**	**OH**	**IH**	**OH**	**IH**	**OH**
S1	-0.194	-1.386	-0.703	-2.496	-0.006	5.010	1.826	-0.310
S3	-7.887	-4.042	-19.010	-21.834	-3.453	-8.443	-0.200	-2.784
	INH1	**ONH1**	**INH1**	**ONH1**	**INH1**	**ONH1**	**INH1**	**ONH1**
S1	1.903	9.949	-0.663	-3.330	0.132	-3.132	13.354	13.326
S3	-0.784	0.762	-18.426	-21.273	-1.913	-4.060	1.510	1.114
	INH2	**ONH2**	**INH2**	**ONH2**	**INH2**	**ONH2**	**INH2**	**ONH2**
S1	1.956	10.390	-0.685	-3.649	0.131	-3.403	13.049	13.450
S3	-0.726	0.787	-18.815	-23.117	-1.906	-4.333	1.433	1.258

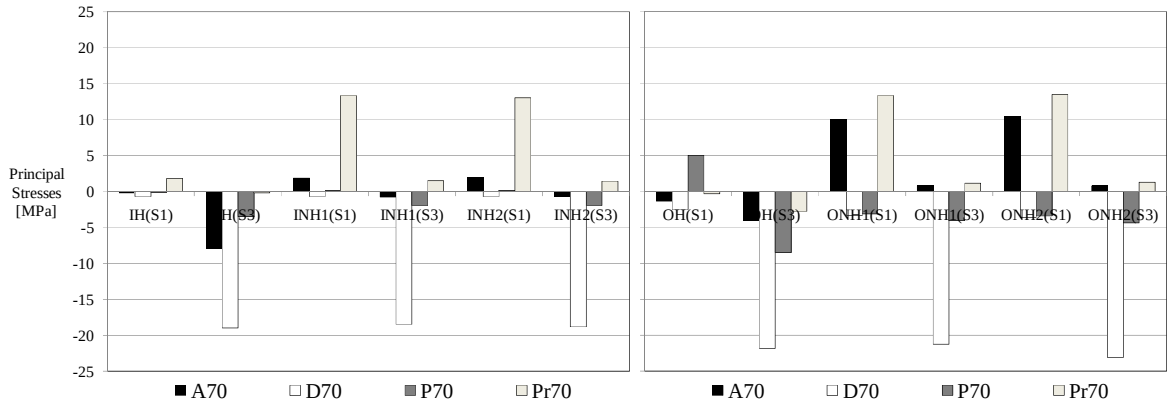

Fig. 7 Principal stresses in cortical zone (I) for isotropic and orthotropic model.

For inclined plane (I), with the values of table 9 or figure 9, a compressive state stress in distal femur part is also visible. Tensile state stresses exist in proximal femur zone. In anterior plan, high values of tensile stress were obtained with orthotropic model. Homogeneous model (IH or OH) has different values, in comparison with inhomogeneous models (INH or ONH), for each mechanical properties used.

CONCLUSIONS

The research presented in this work wants essentially define a finite element model of human femur, which simulate the geometry and different bone mechanical properties, isotropic and orthotropic. The computing of bone mechanical properties has been done using simple exponential equations, in function of measured bone density. The influence of mechanical properties, due different bone density, modifies the numerical results significantly. The maximum values of stresses are in distal and medial zone of femur, due essentially of compressive stress state. The relevance of the mechanical properties, under bone density influence, is a greater importance in this study. The results obtained with orthotropic materials, were lesser than when using isotropic properties. The orthotropic model realizes a more uniform stress distribution in the bone.

REFERENCES

Baca V., Horak Z., Mikulenka P., Dzupa V. Comparison of an inhomogeneous orthotropic and isotropic material models used for FE analyses, Medical Engineering & Physics, 30; 2008 pp.924-930.

M.E. Taylor, K.E. Tanner, M.A.R. Freeman, A.L. Yettram. Stress and strain distribution within the intact femur: compression or bending?, Medical Engineering Physics, 18; 2; 1996 pp.122-131(10).

G. Bergmann, G. Deuretzbacher, M. Heller, F. Graichen, A. Rohlmann, J. Strauss, G.N. Duda. Hip contact forces and gait patterns from routine activities, Journal of Biomechanics, 34; 7; 2001 pp. 859-871.

J.A. Simões, M.A. Vaz, S. Blatcher, M. Taylor. Influence of head constrain and muscle forces on the strain distribution within the intact femur, Medical Engineering and Physics, 22; 7; 2000 pp.453-459.

Peng L., Bai J., Zeng X., Zhou Y. Comparison of isotropic and orthotropic material property assignments on femoral finite element models under two loading conditions, Medical Engineering Physics, 28; 2006 pp.227-233.

Augat P., Schorleimmer S. The role of cortical bone and its microstructure in bone strength, Age and Ageing, 35; S2; 2006 pp.ii27-S2ii31.

Kourtis L.C., Carter D.R., Kesari H., Beaupre G.S. A new software tool (VA-BATTS) to calculate bending, axial, torsional and transverse shear stresses within bone cross section having inhomogeneous material properties, Computer Methods in Biomechanics and Biomedical Engineering, 11; 5; 2008 pp.463-476.

web page: //en.wikipedia.org/wiki/Hounsfiel_units

Alho A., Hoiseth A., Husby T. Bone-mass distribution in the femur, Acta Orthopaedica Scand, 60; 1; 1989 pp.101-104.

Taylor W.R., Roland E., Ploeg H., Hertig D., Klabunde R., Warner R., Hobatho M.C., Rakotomanana L., Clift S.E. Determination of orthotropic bone elastic constants using FEA and modal analysis, Journal of Biomechanics 35; 2002 pp.767-773.

ORGANIZATION

Faculty of Engineering, University of Porto

LOCAL ORGANIZING COMMITTEE

J.F. Silva Gomes and Shaker A. Meguid

(*Co-Chairs*)

Carlos C. António, José M. Cirne, Rui M. Guedes, Paulo G. Piloto
M. Teresa Restivo, Aarash Sofla, Mário A.P. Vaz

INTERNATIONAL SCIENTIFIC COMMITTEE

Clito F. Afonso, *Portugal*; Anabela C. Alves, *Portugal*; C.C. António, *Portugal*; Rui C. Barros, *Portugal*; K.J. Bathe, *USA*; R. de Borst,*Netherlands*; Pedro Camanho, *Portugal*; Carlos Cardeira, *Portugal*; Catarina Castro, *Portugal*; J.L. Chenot, *France*; *Luisa Costa*, Portugal; Álvaro Cunha, *Portugal*; S. Datta, *USA*; J. Rodrigues Dias, *Portugal*; José L. Esteves, *Portugal*; A.J.M. Ferreira, *Portugal*; Elza Fonseca, *Portugal*; Hossam A. Gabbar, *Canada*; S.V. Hoa, *Canada*; I. Hutchings,*UK*; N. Jones, *UK*; Renato N. Jorge, *Portugal*; David Kennedy, *Ireland*; H.W. Klein, *Germany*; M. Langseth, *Norway*; T. Laursen,*USA*; Celina P. Leão, Portugal; R. Lewis, *UK*; D.G. Lee, *Korea*; Nuno Maia, *Portugal*; A. Mal, *USA*; A.T. Marques, *Portugal*; J. Couto Marques, *Portugal*; Alberto Meda, *Italy*; S. A. Meguid, *Canada*; R.E. Miller, *Canada*; G. Mimmi, *Italy*; Rosa M. Miranda, *Portugal*; Y. Miyano, *Japan*; Amiram Moshaiov, *Israel*; Marcelo F. Moura, *Portugal*; Carlos Navarro, *Spain*; C. Papalettere, *Italy*; Paulo Piloto, *Portugal*; J.N. Pires, *Portugal*; J.N. Reddy, *USA*; M.T. Restivo, *Portugal*; Nuno F. Rilo, *Portugal*; J. Dias Rodrigues, *Portugal*; C.Q. Ru, *Canada*; Arlindo J. Silva, *Portugal*; Lucas F.M. Silva, *Portugal*; J.F. Silva Gomes, *Portugal*; C.A. Sciammarella, *Italy*; Jorge H.O. Seabra, *Portugal*; M. Gameiro Silva *Portugal*; S. Carmo Silva *Portugal*; C. M. Soares, *Portugal*; Afzal Suleman, *Portugal*; João M.R.S. Tavares, *Portugal*; M.J . Tooren, *Netherlands*; K.T. Tan, *Singapore*; Mário P. Vaz, *Portugal*; George Weng, *USA*; Y.C. Yoon, *Singapore*; Z. Zhang, *China*.

SYMPOSIA COORDINATORS

Clito Afonso *(U. Porto, Portugal)*, Carlos C. António *(U. Porto, Portugal)*, Tiago Barbosa *(IPB, Portugal)*, Rui C. Barros *(U. Porto, Portugal)*, Pedro Camanho *(U. Porto, Portugal)*, J. Reis Campos *(U. Porto, Portugal)*, M. Braz César *(IPB, Portugal)*, J. Rodrigues Dias *(U. Évora, Portugal)*, José S. Esteves *(U. Porto, Portugal)*, Paulo Fernandes *(IST, Portugal)*, António Ferreira (U. Porto, Portugal), Elza Fonseca *(IPB, Portugal)*, Mihail Fontul *(IST, Portugal*, Hossam Gabbar *(UOIT, Canada)*, J.F. Silva Gomes *(U. Porto, Portugal)*, Renato N. Jorge *(U. Porto, Portugal)*, Jackie Li *(CUNI, USA)*, F. Jorge Lino *(U. Porto, Portugal)*, Ramiro Martins *(INEGI, Portugal)*, Alberto Meda *(U. Rome, Italy)*, Shaker A. Meguid *(U. Toronto, Canada)*, Rosa Miranda *(FCT/UNL, Portugal)*, Paulo Piloto *(IPB, Portugal)*, M. Teresa Restivo *(U. Porto, Portugal)*, Nuno Rilo *(U. Coimbra)*, J. Dias Rodrigues *(U. Porto, Portugal)*, Carla Roque *(U. Porto, Portugal)*, Jorge Seabra *(U. Porto, Portugal)*, Arlindo Silva *(IST, Portugal)*, Lucas F. Silva *(U. Porto, Portugal)*, Aarash Sofla *(U. Toronto, Canada)*, João M. Tavares *(U. Porto, Portugal)*, César Vasques *(INEGI, Portugal)*, Mário A.P. Vaz *(U. Porto, Portugal)*, Zheng Hong Zhu *(York U., Canada)*.

back to top of page

Proceedings IRF'2009
3rd International Conference on
Integrity, Reliability and Failure
Edições INEGI
INEGI-Instituto de Engenharia Mecânica e Gestão Industrial
Rua Dr. Roberto Frias, s/n, 4200-465 Poro, Portugal
Tel:+351 22 957 87 10; *E-mail*: inegi@inegi.up.pt
www.inegi.up.pt
ISBN: 978-972-8826-21-5